

# Highly Transparent Conductive Sheet by Self-assembled Silver Network Electrodes with Antireflective Coating via Roll-to-Roll Process

K. Fujimoto, K. H. Kyung and S. Shiratori

Faculty of Science and Technology, Keio University, 3-14-1 Hiyoshi, Kohoku-ku, Yokohama 223-8522, Japan

**Abstract.** A highly transparent conductive film was fabricated using self-assembled silver electrodes with anti-reflection (AR) film. The micro pore diameter of silver nanoparticles (ca 50~60nm in diameter) network electrodes expanded to size of 200-300  $\mu\text{m}$  by the increase of air voids with evaporated water. The transmittance of the silver network electrode increased was drastically increased by the optical interference from the AR film on the surface and it showed a maximal value 84% (sheet resistance: 8.0  $\Omega/\square$ ). The surface resistance of silver network electrodes films did not change even after coating with the AR films because thickness of AR films (ca 100~200 nm) are extremely thin compared with the diameter of the silver wire (ca 3  $\mu\text{m}$ ). High performance transparent conductive film for electric and optical device was successfully fabricated by roll to roll layer-by-layer (LBL) process.

## 1 Introduction

Self-assembly processes have been well known as one of the effective method for preparing nanoscale multilayer films from molecular scale to microscale by a bottom-up approach. Recently, self-assembly coating technologies have been used to prepare electronic and optical devices under convenient conditions (room temperature and standard pressure) without requiring vacuum processing [1-11]. Moreover, Layer-by-layer (LBL) self-assembled multilayer films are constructed from various nano scale order materials on three dimensional substrates such as optical lenses [12], particles [13] and mesh substrate [14]. And it can fabricate functional nano structural film via roll-to-roll process [15-17]. Up to nowadays, most of the transparent conductive films are indium tin oxide (ITO) film which used rare metal, and produced using vacuum processing. Therefore, it is expected for the practical realization of transparent conductive film by simple wet process without using vacuum process. In this research, we report the fabrication of transparent conductive films by self-assembly of silver nano particles to form the microscale network electrode with the deposition of anti-reflection (AR) film to increase the transparency of visible light.

## 2 Experimental procedure

The dispersed silver nanoparticles solution was obtained from Cima NanoTech [18-20]. The concentrations of silver emulsions were adjusted 1 and 0.8 wt% in

toluene/H<sub>2</sub>O, it was ultrasonically shaken for 10 min. These silver emulsions was casting on PET film and formed thin films by bar coating method. Fig 1 shows schematic illustrations to form highly transparent conductive film using self-assembled silver nanoparticles network electrodes with AR film.

Poly(diallyldimethylammonium chloride) (PDDA) were used as the positively charged polyelectrolyte. Aqueous solutions of Titanium (IV) bis-(ammonium lactate) dihydroxide (TALH), Sodium Silicate (Na<sub>2</sub>SiO<sub>3</sub>), and SiO<sub>2</sub> nanoparticles were used as the negatively charged solutions. Single-block AR as (PDDA/SiO<sub>2</sub>)<sub>8</sub> and double-block AR as (PDDA/TALH)<sub>20</sub>/(PDDA/Na<sub>2</sub>SiO<sub>3</sub>)<sub>40</sub> coated on silver network electrode using LBL method [3-17]. Here, (A/B)<sub>n</sub> indicate that A is used as cation, B is used as anion and 1 (A/B) layer-by layer films are deposited n bilayers.

Single-block AR film was deposited by PDDA and SiO<sub>2</sub> solutions and intermediate H<sub>2</sub>O rinsing 3 times for 8 cycles on silver network electrode. Double-block AR was deposited by PDDA and TALH solutions and intermediate H<sub>2</sub>O rinsing for 3 times for 20 cycles on silver network electrode. The fabricated (PDDA/TALH)<sub>20</sub> films were used as the higher-refractive-index layer. After the deposition of the higher-refractive index layer, (PDDA/Na<sub>2</sub>SiO<sub>3</sub>)<sub>40</sub> layers were deposited by dipping the substrate into PDDA and Na<sub>2</sub>SiO<sub>3</sub> solutions and H<sub>2</sub>O rinsing bath 3 times and in total repeated for 40 cycles.

The film thickness and refractive indexes were estimated by an ellipsometer. The sheet resistance was

measured by four terminal probe units. The optical properties were estimated using an ultraviolet–visible (UV–vis) spectroscopy and Haze mater. The surface morphologies were measured by Laser microscopy.

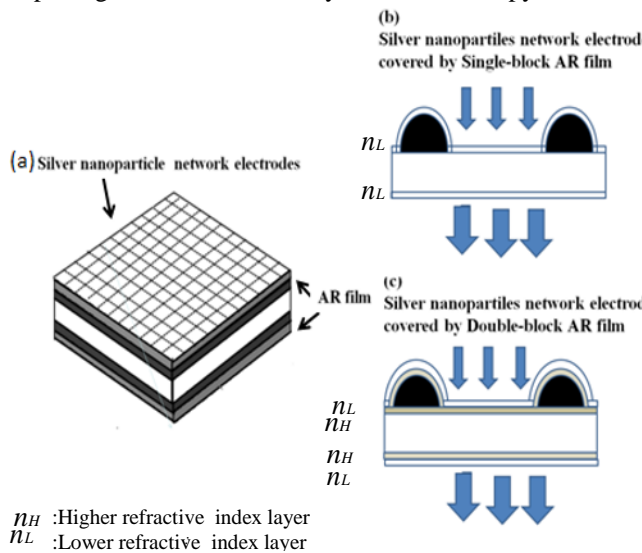


**Fig. 1.** Schematic image of A highly transparent conductive film was fabricated using self-assembled silver network electrodes with anti-reflection (AR) film.

### 3. Results and discussion

#### 3.1 Self-assembled micro structural silver nanoparticles network electrodes

The micro structural network electrode was fabricated by self assembly of the silver nanoparticles emulsified solutions. Table 1 shows the values of sheet resistance and transmittance of the fabricated silver nanoparticles network electrodes with the emulsified solution conditions. As shown in this table, it was clearly shown that sheet resistance was lower when the silver concentration was the higher ((a)<(c), (b)<(d)). For example, by comparing (b) and (d), the transmittance of (d) increased 3% by increasing the silver concentration. On the other hand, transmittance of the film was higher, when the ratio of water to dispersion was higher in the solution ((b)>(a), (d)>(c)).

**Table 1.** Sheet resistance and transmittance of silver network electrode at the silver solution conditions

Silver concentration (%)	Dispersion: Water	Sheet resistance ( $\Omega/\square$ )	Transmittance (%)
(a) 1	2:1	12.7	65.5
(b) 1	7:4	14.1	70.3
(c) 0.8	2:1	13.7	66.4
(d) 0.8	7:4	16.4	67.4

Surface morphologies of silver network electrodes at the various silver solution conditions were shown in Fig.2. As show in Fig. 2, the density of silver network electrodes of (b) and (d) are lower than those of (a) and (c). Since toluene quantity of the dispersion of (b) and (d) are

smaller than those of (a) and (c), the size of the voids are larger when the quantity of water is larger

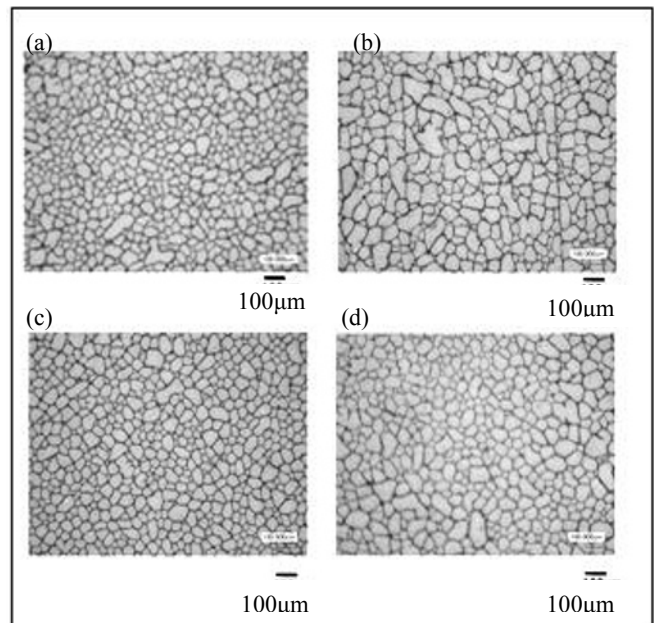


**Fig. 2.** Surface morphologies of silver network electrodes at the various silver solution conditions. (a) Ag 1%, Dispersion: Water = 2:1, (b) Ag 1%, 7:4, (c) Ag 0.8 %, 2:1, (d) Ag 0.8 %, 7:4

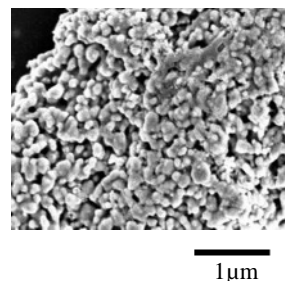


**Fig. 3** SEM image of silver network electrode composed of numerous silver nanoparticles.

As show in the photos, the diameter of micro pores were distributed from the size of 200 to 300  $\mu\text{m}$  by the the increase of air voids formed by the water evaporation.

We consider this phenomenon was caused by the difference of evaporation speed of toluene and water. When the solution evaporation speed is higher, the smaller voids are formed, and when it is lower, the smaller voids are formed.

This was caused also by the affinity difference of silver nanoparticles to the water and toluene. Since the affinity of silver nanoparticles is larger for toluene and smaller for water, phase separated water droplets do not contain silver nano particles. And these phase separated water droplets forms the circle shape voids among the silver wire of the network that were formed by the assembly of silver nanoparticles. The narrow view of silver wire was shown in Fig.3. As shown in the figure, each silver network was composed of selfassembled silver nanoparticles.

Based on these experimental results shown above, it can be said that transmittance and sheet resistance of silver

network electrodes was increased according with the expanding size of microsize air voids appeared after water evaporation. [18-20].

3. 2 . Self-assembled nano heterostructural anti-reflection film

The refractive index and film thickness of a double-block AR film are estimated using eqs. (1)–(5) [2], where  $n_0$  is the refractive index of the air medium,  $n_1$  is the refractive index of the lower-refractive-index layer,  $n_2$  is the refractive index of the higher-refractive-index layer,  $d$  is the film thickness of AR film, and  $\lambda$  is wavelength of incident light.

$$n_1 = (n_0 n_s)^{0.5} \quad (1)$$

$$n_1^3 = n_0^2 n_s \quad (2)$$

Double-block AR

$$n_1^3 = n_0^2 n_s \quad (3)$$

$$n_1 = n_2^{0.5} \quad (4)$$

$$nd = \lambda / 4 \quad (5)$$

In this experimet, refractive index and film thickness of higher and lower refractive index layers were adjusted by the deposition cycles of LBL process.

Table 2 shows refractive indexes and film thicknesses of (PDDA/SiO<sub>2</sub>)<sub>8</sub>, (PDDA/TALH)<sub>20</sub> and (PDDA/Na<sub>2</sub>SiO<sub>3</sub>)<sub>40</sub> coated on silicon wafer measured by 632.5 nm of incident light wavelength were estimated by ellipsometer [21, 22]. On the other hand, the calculated value of the refractive index and film thickness obtained from the equations (1) to (5) was shown in Table 3.

Table 2. The refractive indexes and film thickness of fabricated

	Refractive index	Film thickness (nm)
(PDDA/SiO <sub>2</sub> ) <sub>8</sub>	1.30	109
(PDDA/TALH) <sub>20</sub>	1.75	80
(PDDA/Na <sub>2</sub> SiO <sub>3</sub> ) <sub>40</sub>	1.47	92

films measured by ellipsometry.

Table 3. Calculated film thickness based on the equations (1) ~ (5).

	Refractive index	Film thickness (nm)
(PDDA/SiO <sub>2</sub> ) <sub>8</sub>	1.30	106
(PDDA/TALH) <sub>20</sub>	1.75	78
(PDDA/Na <sub>2</sub> SiO <sub>3</sub> ) <sub>40</sub>	1.47	90

By comparing these two tables, the refractive indexes and film thicknesses of the (PDDA/SiO<sub>2</sub>)<sub>8</sub> film was consistent with the results obtained using eqs. (1)–(2) for a single-block AR film, and the refractive indexes and film thicknesses of the (PDDA/TALH)<sub>20</sub> and (PDDA/Na<sub>2</sub>SiO<sub>3</sub>)<sub>40</sub> films were consistent with the values obtained using eqs. (3)–(5) for a double-block AR film.

Fig 4 shows the transmittance spectra of single-block AR films and silver network electrode with AR films.

These spectra were measured by a UV–vis spectrometer using 300 to 1000 nm of incident light wavelength. The mean value of the transmittance of single-block AR film was 96 % in the visible range (400 ~ 700nm). The transmittance of silver nanoparticles network electrode was increased when it is covered with single-block AR film, and it showed maximal value of 79 % in the visible range.

Fig. 5 shows the transmittance spectra of double-block AR films and silver network electrode with AR films. The transmittance of double-block AR films showed 99 % maximum transmission in the visible range. The transmittance of silver network electrode was increased when it is covered with double-block AR film, and it showed maximal value 84 % in the visible range. This increasing transmittance of silver network electrode was affected by optical interference from AR film. The transmittance of silver network electrode covered by double-block AR was higher than that covered by single-block AR film.

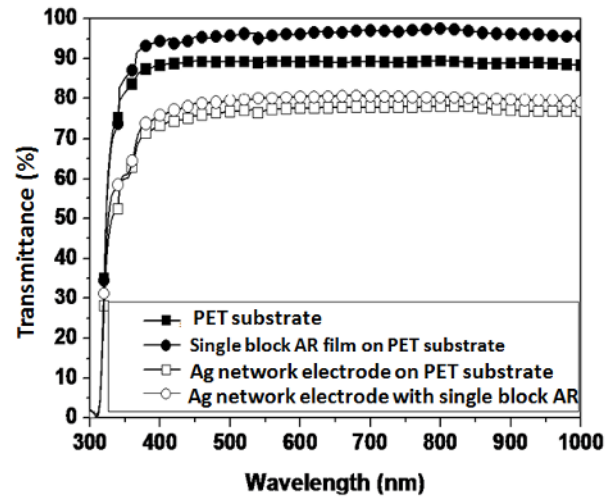


Fig. 4 Transmittance of silver network electrode with single block AR film

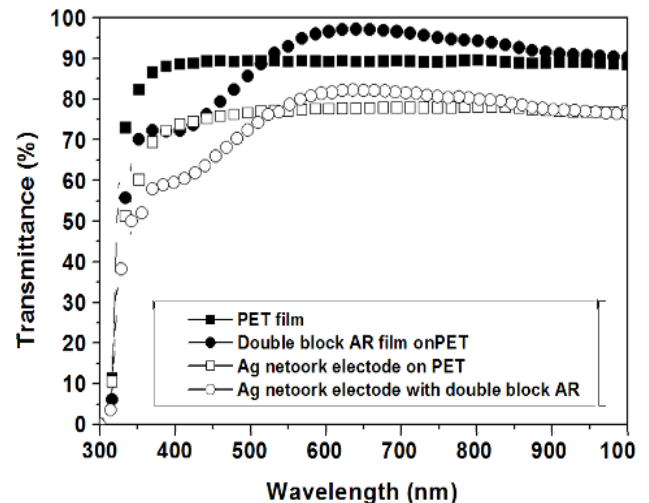


Fig. 5 Transmittance of silver network electrode with double block AR film

As shown in Fig.3, the transittance of single-block AR film was lower than that of double-block AR films which

are shown in Fig.4. We consider that this is because of the surface aggregation of  $\text{SiO}_2$  particles on silver network electrode for the single-block AR film. On the other hand, double-block AR films formed by (PDDA/TALH)<sub>20</sub> and (PDDA/ $\text{Na}_2\text{SiO}_3$ )<sub>40</sub> films shows smoother surface and the higher transmission compared with the single-block AR film because TALH and  $\text{Na}_2\text{SiO}_3$  forms less aggregation owing to the low speed film deposition based on the precursor.

The surface resistance of silver network electrodes films did not change despite coated with AR films. It is considered that surface resistance was slightly shifted because the thickness of AR films (ca 100~200 nm) are too thin compared with the diameters (ca 3  $\mu\text{m}$ ) of silver network electrodes.

Fig. 6 shows the photograph of highly transparent conductive film was fabricated by roll-to-roll process. Anti-reflection coating silver network electrode film was observed blue interfering light under fluorescent light as shown in Fig. 5. It is confirmed by the inhabiting reflection of silver network electrode film. As shown in the figure, English characters were clearly shown through the film. The transmittance and sheet resistance of highly transparent conductive film was 84 % and 8.0  $\Omega/\square$ , respectively. It is concluded that self-assembled micro silver network electrode and nano structural anti-reflection films were uniformly coated on PET film via layer-by-layer roll-to-roll process.

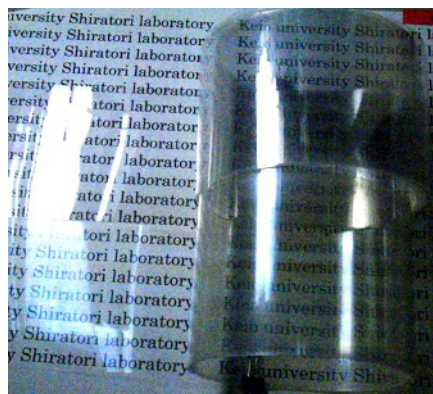


**Fig. 6.** Highly transparent conductive sheet by self-assembled silver electrode with AR film (under side) and without AR film (upper side).

#### 4. Conclusions

In this paper, we reported highly transparent conductive film, which has self-assembled silver network electrode and anti-reflection film. The enhancement transmittance of silver electrodes was confirmed by the adjustment of microstructure of silver network and anti-reflective interference. Moreover, self-assembled highly transparent conductive film was successfully fabricated by a roll-to-roll LBL-SA process. The surface resistance of silver network electrodes films did not change despite coated with AR films. It is considered that surface resistance slightly shift because thickness of AR films are too thin compared with the film thickness and width of silver nanoparticles network electrodes. The

transmittance and sheet resistance of highly transparent conductive film was 84 % and 8.0  $\Omega/\square$ , respectively. These experimental results obtained in this research suggest that high performance transparent conductive film was successfully obtained by the proposed method that can be used for electric and optical devices.

#### Acknowledgements

A part of this study was supported by the financial aid from JST A-STEP AS2211182B. The authors are also grateful to Mr. Nakata and Mr. Yamane of Toda Kogyo Corp. for the predation of silver network electrode.

#### References

1. K. Ariga, J. P. Hill, and Q. Ji: *Phys. Chem. Chem. Phys.* **9** 319, 2, (2007)
2. M. Shimomura and T. Sawadaishi: *Curr. Opin. Colloid Interface Sci.* **6** (2001) 11
3. G. Decher, J. D. Hong, and J. Schmitt: *Thin Solid Films* 210–211, 831, (1992).
4. G. Decher: *Science* **277**, 1232, (1997)
5. S. S. Shiratori and M. F. Rubner *Macromolecules* **33**. 4213, (2000)
6. W. Chen and T. J. McCarthy, *Macromolecules* **30**, 78. (1997)
7. F. Shi, Z. Wang, and X. Zhang: *Adv. Mater.* **17**, 1005 (2005).
8. G. H. Zeng, J. Gao, S. L. Chen, H. Chen, Z. Q. Wang, and X. Zhang, *Langmuir* **23** 11631 (2007).
9. T. Ito, Y. Okayama, and S. Shiratori: *Thin Solid Films* **393** (2001) 138.
10. S. Fujita and S. Shiratori, *Jpn. J. Appl. Phys.* **43** (2004) 2346.
11. J. H. Kim, S. Fujita, and S. Shiratori, *Colloids Surf. A* **284–285** (2006) 290.
12. K. Fujimoto, K. H. Kyung, and S. Shiratori, *Jpn. J. Appl. Phys.* **50** (2011) 045803
13. G. Schneider and G. Decher, *Nano Lett.* **4**, 1833, (2004)
14. M. Matsuda and S. Shiratori, *Langmuir*, **27**, 4271 (2011)
15. S. Shiratori: *Japan Patent* 3262323 (2001).
16. K. Fujimoto, S. Fujita, B. Ding, and S. Shiratori, *Jpn. J. Appl. Phys.* **44**, L126, (2005)
17. K. Fujimoto, J. H. Kim and S. Shiratori *Jpn. J. Appl. Phys.* **47**, 8644, (2008)
18. A. Garbar, F. De La Vega, E. Matzner, C. Sokolinsky, V. Rosenband, A. Kiselev, D. Lekhtman, *US Patent* 7736693
19. A. Garbar, C. Rottman, F. De La Vega, J. Brodd, *US Patent* 8105472
20. <http://cimananotech.com>
21. H. A. Macleod: *Thin Film Optical Filters* (Macmillan, New York, 36 (1986)
22. F. Abeles: *Ann. Phys. (Paris)* **5**,706 (1950)